PROCEEDINGS OF SCIENCE

(g-2) and SIMP dark matter: implications to collider

Sarif Khan*

Institut für Theoretische Physik, Georg-August-Universität Göttingen, Friedrich-Hund-Platz 1, 37077 Göttingen, Germany

E-mail: sarif.khan@uni-goettingen.de

In this work, we have tried to explain a few unsolved beyond standard model problems namely electron and muon $(g-2)$, neutrino mass and dark matter. Moreover, we have also explained the implications of the involved particles at the collider. For this purpose, in the present work, we have proposed a suitable extension of the minimal $L_\mu - L_\tau$ model to address the aforementioned drawbacks of SM. In our model, a new Yukawa interaction involving electrons, a singlet vector-like fermion $(\chi^\pm)$ and a scalar (either a complex singlet Φ_4' or an $SU(2)_L$ doublet Φ_2') provides the additional one loop contribution to electron (g-2). On the other hand $(g-2)_\mu$ can be satisfied with the $Z_{\mu\tau}$ gauge boson. The judicious choice of $L_\mu - L_\tau$ charges of the additional fields make the gauge model anomaly free. The lightest component among the neutral parts of the additional scalar fields is a DM candidate freezes out by the $3 \to 2$ processes. Our DM can also be detected at the direct detection experiments mediated by the SM Z boson and the process is suppressed by the $Z - Z_{\mu\tau}$ mixing angle. We have also satisfied the bound from DM relic density, unitarity and self-interaction of DM which are applicable to the present DM study. Finally, our proposed model can also be tested at the future lepton collider through the process $e^+e^- \to \chi^+\chi^- \to e^+e^-\cancel{E}_T$.

41st International Conference on High Energy physics - ICHEP2022
6-13 July, 2022
Bologna, Italy

*Speaker

PoS(ICHEP2022)268

1. Introduction

As we are sure that the standard model (SM) is not the complete theory of nature because it can not explain several phenomena namely dark matter, neutrino mass and also can not explain the anomalies in electron and muon $(g-2)$. In explaining all the aforementioned phenomena, we have extended the SM particle content and also the gauge content of the SM gauge group. In particular, we have extended the fermion sector with one vector-like fermion singlet with nonzero hypercharge and the scalar sector with three additional scalars. Among them, one is $SU(2)_L$ doublet and the other two are singlets. On the other hand, the gauge group has been extended by an abelian gauge group $U(1)_{L_\mu - L_\tau}$. Among the two scalars that do not acquire vacuum expectation values (VEVs) mix each other. The lightest among the neutral components becomes a stable DM candidate which freezes out by the $3 \to 2$ processes and in the literature, this type of DM is called a self-interacting massive particle (SIMP) dark matter. The extra charge fermions help in explaining the $(g-2)_e$ and are a very interesting signal at the e^+e^- collider. The additional singlet scalar which acquires mass has the $U(1)_{L_\mu - L_\tau}$ charge and imparts mass to the extra gauge boson which explains the $(g-2)_\mu$. In studying DM, we have looked for all the possible bounds which can arise in our study namely the DM relic density bound, DM self-interaction of DM and Unitarity bound. Moreover, we have also checked that our DM is relatively safe from the direct detection experiments. One interesting aspect of the present study is that due to the lightness of the SIMP DM after satisfying all the bounds, we get enhancement in the production of the additional charge fermions because they are produced by the $t-$channel processes mediated by the light SIMP DM. Finally, for a detailed study of the present work we refer the reader to look at Ref. [1].

2. Extended $L_\mu - L_\tau$ Model

The present model is discussed in detail in Ref. [1]. In Tab. 1 and Tab. 2, we have shown the complete particle spectrum and associated charges under the complete gauge group $SU(3)_C \times SU(2)_L \times U(1)_Y \times U(1)_{L_\mu - L_\tau}$ of the present model. Here we would like to note that since all fermions are vector-like under the $L_\mu - L_\tau$ symmetry the extended model is also anomaly free as it was for the minimal model.

Gauge	Baryon Fields			Lepton Fields					Scalar Fields			
Group	$Q_L^i = (u_L^i, d_L^i)^T$	u_R^i	d_R^i	$L_L^i = (\nu_L^i, e_L^i)^T$	e_R^i	N_R^i	χ_L	χ_R	Φ_1'	Φ_2'	Φ_3'	Φ_4'
$\mathrm{SU(2)_L}$	2	1	1	2	1	1	1	1	2	2	1	1
$\mathrm{U(1)_Y}$	1/6	2/3	−1/3	−1/2	−1	0	−1	−1	1/2	1/2	0	0

Table 1: Particle contents and their corresponding charges under the SM gauge group.

Gauge	Baryonic Fields	Lepton Fields					Scalar Fields			
Group	(Q_L^i, u_R^i, d_R^i)	(L_L^e, e_R, N_R^e)	$(L_L^\mu, \mu_R, N_R^\mu)$	$(L_L^\tau, \tau_R, N_R^\tau)$	χ_L	χ_R	Φ_1'	Φ_2'	Φ_3'	Φ_4'
$\mathrm{U(1)}_{L_\mu - L_\tau}$	0	0	1	−1	1/3	1/3	0	−1/3	1	−1/3

Table 2: $L_\mu - L_\tau$ charges for fermions and scalars of the present model.

The full Lagrangian of the present model is given by

$$\mathcal{L} = \mathcal{L}_{\rm SM} - \frac{1}{4}\hat{X}_{\alpha\beta}\hat{X}^{\alpha\beta} + \frac{\epsilon}{2}\hat{X}_{\alpha\beta}\hat{B}^{\alpha\beta} - g_{\mu\tau}\sum_{\substack{\ell=\mu,\nu_\mu,\\ \tau,\nu_\tau}} Q^{\ell}_{\mu\tau}\bar{\ell}\gamma^{\alpha}\ell\hat{X}_{\alpha} + \Bigg[i\,\bar{\chi}\partial\!\!\!/\chi - \bar{\chi}\gamma^{\alpha}\chi\left(\frac{g_{\mu\tau}}{3}\hat{X}_{\alpha} - g_1\hat{B}_{\alpha}\right)$$
$$-M_{\chi}\overline{\chi}\chi - \left(\beta^{R}_{e\chi}\overline{L_e}\Phi'_2\chi_R + \beta^{L}_{e\chi}\overline{e_R}\,\chi_L\Phi'_4 + h.c.\right)\Bigg] + \mathcal{L}_N + \sum_{i=2}^{4}\left(D_{\alpha}\Phi'_i\right)^{\dagger}\left(D^{\alpha}\Phi'_i\right) - \mathcal{V}(\Phi'_1,\Phi'_2,\Phi'_3,\Phi'_4)\,. \tag{1}$$

The terms within the square brackets represent the Lagrangian of vector-like fermion χ including the new Yukawa interactions with couplings $\beta^{R}_{e\chi}$ and $\beta^{L}_{e\chi}$ respectively. The Lagrangian for three right-handed neutrinos is denoted by $\mathcal{L}_N$. We have written the exact form of $\mathcal{L}_N$ below.

$$\begin{aligned}\mathcal{L}_N &= \frac{i}{2}\sum_{\substack{i=e,\mu,\\ \tau}}\overline{N_i}\partial\!\!\!/N_i + \sum_{\substack{i=e,\mu,\\ \tau}}\left(y_{ii}\,\overline{L_i}\Phi'_1 N_i + h.c.\right) + \big(M_{ee}N_eN_e + h_{e\mu}N_eN_{\mu}\Phi'^{\dagger}_3 \\ &\quad + h_{e\tau}N_eN_{\tau}\Phi'_3 + M_{\mu\tau}e^{i\theta}N_{\mu}N_{\tau} + h.c.\big)\,,\end{aligned} \tag{2}$$

where the first term is the kinetic term of N_i while the rest are interaction terms responsible for the light neutrino mass generation via the Type-I seesaw mechanism. Finally, the last two terms in Eq. 1 are the kinetic and interaction terms for the BSM scalars (Φ'_i, i = 2, 3, 4). In the kinetic term, D_{α} is the usual covariant derivative involving gauge boson(s) and generator(s) of each group under which Φ'_i transforms non-trivially. The explicit form of $\mathcal{V}$, invariant under the full gauge group is given below

$$\begin{aligned}\mathcal{V}(\Phi'_1,\Phi'_2,\Phi'_3,\Phi'_4) &= \sum_{i=2}^{4}\left[\mu_i^2\left(\Phi'^{\dagger}_i\Phi'_i\right) + \lambda_i\left(\Phi'^{\dagger}_i\Phi'_i\right)^2\right] + \sum_{i,j,j>i}\lambda_{ij}\left(\Phi'^{\dagger}_i\Phi'_i\right)\left(\Phi'^{\dagger}_j\Phi'_j\right) \\ &\quad + \lambda'_{12}\left(\Phi'^{\dagger}_1\Phi'_2\right)\left(\Phi'^{\dagger}_2\Phi'_1\right) + \left[\mu\left(\Phi'^{\dagger}_1\Phi'_2\right)\Phi'^{\dagger}_4 + \xi\left(\Phi'_3\Phi'^{3}_4\right) + h.c.\right].\end{aligned} \tag{3}$$

Here for necessary vacuum alignment we need $\mu^2_{1,3} < 0$, $\mu^2_{2,4} > 0$ and $\lambda_i > 0$. The second condition, $\mu^2_{2,4} > 0$, ensures that two new $L_{\mu} - L_{\tau}$ charged scalars Φ'_2 and Φ'_4 do not have any VEVs. After both EWSB and $L_{\mu} - L_{\tau}$ breaking, the 2×2 mass matrix for the neutral component of Φ'_2 (ϕ'_2) and Φ'_4 is given by

$$M^2_{\phi'_2-\Phi'_4} = \begin{pmatrix} a & b \\ b & c\end{pmatrix}\,. \tag{4}$$

where $a = \mu_2^2 + (\lambda_{12} + \lambda'_{12})\frac{v^2}{2} + \lambda_{23}\frac{v_{\mu\tau}}{2}$, $c = \mu_4^2 + \lambda_{14}\frac{v^2}{2} + \lambda_{34}\frac{v_{\mu\tau}}{2}$ and $b = \frac{\mu v}{\sqrt{2}}$. One can easily diagonalise the above mass matrix using an orthogonal transformation by an angle θ_D and the resultant eigenstates are related to the old basis sates (ϕ'_2, Φ'_4) in the following way

$$\begin{pmatrix}\phi_2\\ \phi_4\end{pmatrix} = \begin{pmatrix}\cos\theta_D & -\sin\theta_D\\ \sin\theta_D & \cos\theta_D\end{pmatrix}\begin{pmatrix}\phi'_2\\ \Phi'_4\end{pmatrix}, \tag{5}$$

where, the mixing angle θ_D can be expressed in terms of the parameters of the Lagrangian as,

$$\begin{aligned}\theta_D &= \frac{1}{2}\tan^{-1}\left(\frac{2b}{c-a}\right), \\ &= \frac{1}{2}\tan^{-1}\left[\frac{\sqrt{2}\,\mu v}{\mu_4^2-\mu_2^2+(\lambda_{14}-\lambda_{12}-\lambda_{12}^{\prime})\frac{v^2}{2}+(\lambda_{34}-\lambda_{23})\frac{v_{\mu\tau}}{2}}\right] \end{aligned} \quad (6)$$

and the masses corresponding to the physical states ϕ_2 and ϕ_4 are described in Ref. [1]. In our work, we have considered that ϕ_4 is the lightest state and is a suitable dark matter candidate.

3. Results

In this section, we are going to discuss our results which were originally presented in Ref. [1]. In particular, for the numerical values of different bounds and the complete set of Boltzmann equations we refer the readers to look at the Ref. [1].

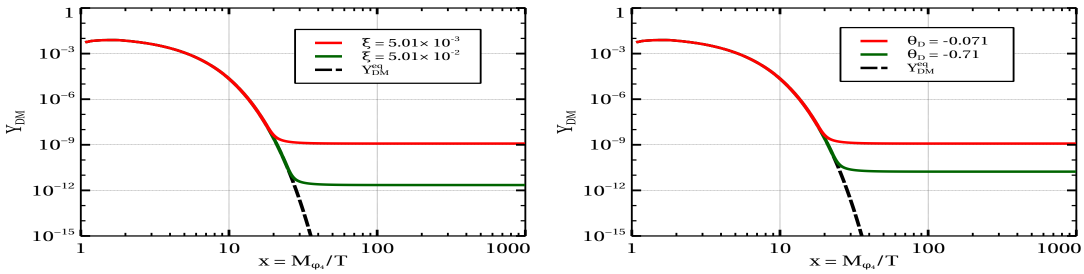

Figure 1: Numerical results: Evolution of $Y_{\rm DM}$ with x for various model parameters like ξ, θ_D.

In the left panel (LP) and right panel (RP) of Fig. 1, we have shown the variation of DM co-moving number density (Y_{DM}) with $x(\frac{M_{\phi_4}}{T})$. In the LP, we have shown the variation with the parameter, ξ and this is directly related to the DM annihilation because of the presence of the cubic term as shown in Eq. 3. In particular, the $3 \to 2$ processes which are the main processes for the DM freezes out are linearly proportional to the parameter ξ which implies that if we increase ξ then we increase the cross-section and it reduces the DM relic density and vice versa. This behaviour is visible in the LP of the figure. On the other hand in the RP also we can see the same kind of behaviour for the mixing angle θ_D.

In the LP of Fig. 2, we have shown the scatter plot in the $M_{\phi_4} - \xi$ plane after satisfying the different bounds. The blue points are obtained after satisfying the DM relic density bound, red points are obtained if we impose the self-interaction bound of DM and finally we obtain the green points after imposing the Unitarity bounds. On the other hand in the RP, we have shown the scatter plots in the $M_{\phi_4} - \frac{\sigma_{self}}{M_{\phi_4}}$ plane. In obtaining the plot, we have only imposed the DM relic density.

In Fig. 3, we have shown the production cross section for $e^+e^- \to \chi^+\chi^-$ process mediated by the DM ϕ_4. In the LP, we have shown the $\chi^+\chi^-$ production for different centre of mass (c.o.m) energy. Since the production cross-section is inversely proportional to the c.o.m energy so with the increment of the c.o.m energy our production cross-section decrease as seen from the figure. We have shown it for two different mass values of χ and the production of $\chi^+\chi^-$ for M_χ = 600 GeV happens only when the collider c.o.m energy crosses the threshold value which 1200 GeV. On the

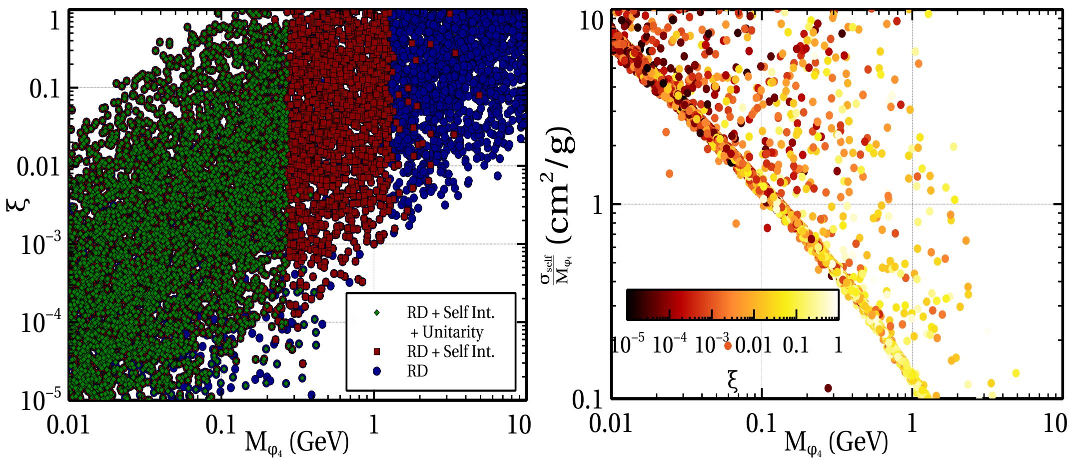

Figure 2: Left panel: Allowed parameter space is $\xi - M_{\phi_4}$ plane for different constraints. Right panel: Variation of $\sigma_{\rm self}/M_{\phi_4}$ with M_{ϕ_4}.

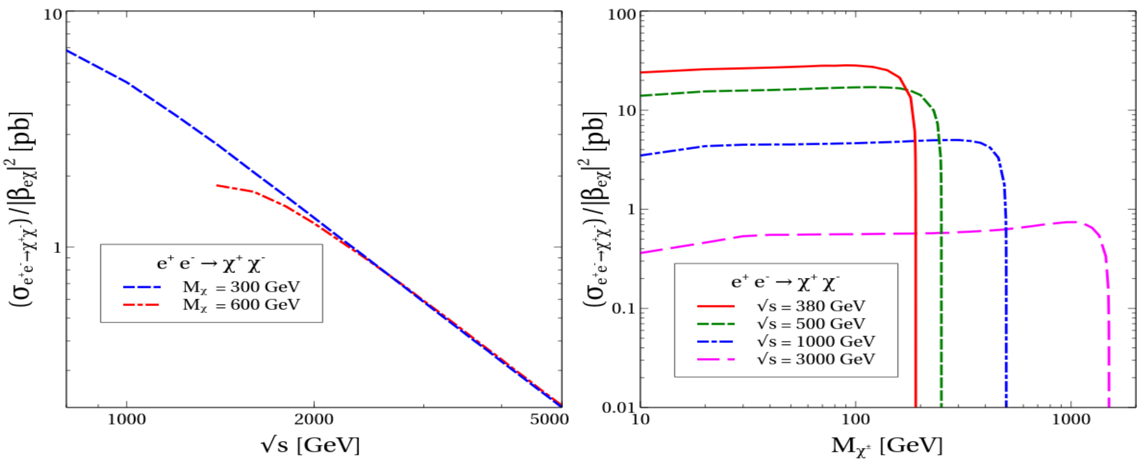

Figure 3: Left panel shows the pair production of χ^+ and χ^- for different c.o.m energy for two values of $\chi^\pm$ mass at the e^+e^- lepton collider. Right panel shows the variation of χ^+ and χ^- production rate with $\chi^\pm$ mass $M_{\chi^\pm}$ for different values of c.o.m. energies.

other hand, in the RP of the same figure, we have shown the $\chi^+\chi^-$ production from the different c.o.m energy for different values of M_χ. We can see that there is a sharp drop in the production cross section when we cross $M_\chi \sim \frac{\sqrt{s}}{2}$. This happens due to the kinematical threshold for the production of $\chi^+\chi^-$.

In the LP and RP of Fig. 4, we have shown the allowed parameter space after satisfying the $(g-2)_e$. The solid and dashed lines correspond to the 3σ and 5σ statistical significance of the $e^+e^-\not{E}_T$ signal over SM backgrounds for the present model. We can see that the parameters which explain the electron $(g-2)$ can be accessed at the e^+e^- collider for very low luminosity values. This kind of signal enhancement is not possible at the pp collider, so we do not have any interesting detection prospects of the present model at the hadron collider.

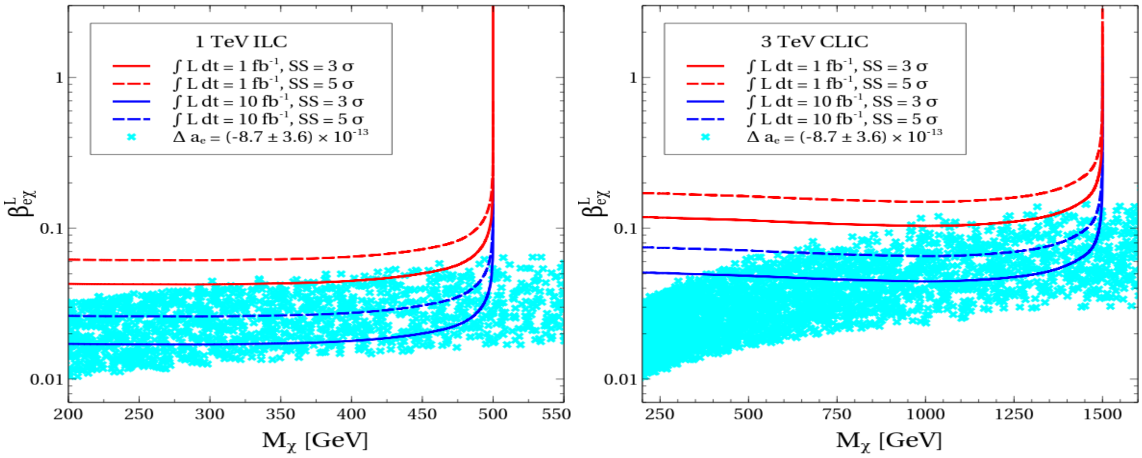

Figure 4: Left and right panels show the allowed regions (by cyan colour points) after satisfying the $(g-2)_e$ in $\beta^L_{e\chi} - M_\chi$ plane for 1 TeV and 3 TeV lepton colliders, respectively. The solid and dashed lines correspond to the variation of 3σ and 5σ statistical significance lines of $e^+e^-\not{E}_T$ signal with the charged singlet fermion mass for the luminosity 1 fb^{-1} and 10 fb^{-1}, respectively. The other parameters kept fixed at $\beta^R_{e\chi} = \beta^L_{e\chi}$, $M_{\phi_4} = 100$ MeV, $\theta_D = 0.1$ and M_{ϕ_2} has been varied between 1 to 10 TeV.

4. Conclusion

In this work, we have extended the general $U(1)_{L_\mu - L_\tau}$ model by a scalar doublet (Φ'_2), a singlet scalar (Φ'_4) and a vector like singlet fermion χ to address the deviations found in the experimental and theoretical values of anomalous magnetic moments for both muon and electron. All these new fields have specific $L_\mu - L_\tau$ charges as required by the new Yukawa interactions and that also cancel the gauge anomaly. We have shown that in the minimal model, considering the present bounds on $Z_{\mu\tau}$ from various experiments particularly from Borexino, it is not possible to address both these anomalies simultaneously. Apart from the one-loop contribution due to the neutral gauge boson $Z_{\mu\tau}$ through mixing, the additional contribution coming from one loop diagrams involving χ and ϕ_2 or ϕ_4 provide the deficit in $(g-2)_e$ as required by the experimental data when the relevant parameters remain within the following range $\beta^L_{e\chi} \gtrsim 5 \times 10^{-2}$, 10^{-3} rad $\lesssim |\theta_D| \lesssim 0.1$ rad and 1 TeV $\leq M_{\phi_2} \leq 10$ TeV. Interestingly, to achieve this, we also have a natural SIMP dark matter candidate ϕ_4, an admixture of Φ'_4 and ϕ'_2 (neutral part of Φ'_2), the signature of which can be found as missing energy at the upcoming e^+e^- linear colliders like ILC and CLIC. The characteristics of the SIMP dark matter are achieved through the number changing $3 \to 2$ processes like $\phi_4\phi_4\phi_4 \to \phi_4^\dagger\phi_4$, $\phi_4^\dagger\phi_4\phi_4 \to \phi_4^\dagger\phi_4^\dagger$. In conclusion, this work tackles several beyond SM problems, namely neutrino mass, dark matter, and anomalies in the electron and muon (g-2) at the same time, with important implications for future collider research.

References

[1] A. Biswas and S. Khan, "*$(g\text{-}2)_{e,\mu}$ and strongly interacting dark matter with collider implications*", JHEP **07**, 037 (2022) [arXiv:2112.08393 [hep-ph]].